

# UC Merced

## UC Merced Previously Published Works

### Title

A full-spectrum k-distribution look-up table for radiative transfer in nonhomogeneous gaseous media

### Permalink

<https://escholarship.org/uc/item/9554d031>

### Authors

Wang, Chaojun  
Ge, Wenjun  
Modest, Michael F  
et al.

### Publication Date

2016

### DOI

10.1016/j.jqsrt.2015.08.017

Peer reviewed



Contents lists available at ScienceDirect

# Journal of Quantitative Spectroscopy & Radiative Transfer

journal homepage: [www.elsevier.com/locate/jqsrt](http://www.elsevier.com/locate/jqsrt)

## A full-spectrum $k$ -distribution look-up table for radiative transfer in nonhomogeneous gaseous media



Chaojun Wang<sup>a,b</sup>, Wenjun Ge<sup>b</sup>, Michael F. Modest<sup>b,\*</sup>, Boshu He<sup>a</sup>

<sup>a</sup> School of Mechanical, Electronic and Control Engineering, Beijing Jiaotong University, Beijing, China

<sup>b</sup> School of Engineering, University of California, Merced, USA

### ARTICLE INFO

#### Article history:

Received 9 June 2015

Received in revised form

30 July 2015

Accepted 26 August 2015

Available online 4 September 2015

#### Keywords:

Radiative heat transfer

Full-spectrum  $k$ -distribution

Look-up table

Accuracy

Efficiency

### ABSTRACT

A full-spectrum  $k$ -distribution (FSK) look-up table has been constructed for gas mixtures within a certain range of thermodynamic states for three species, i.e., CO<sub>2</sub>, H<sub>2</sub>O and CO. The  $k$ -distribution of a mixture is assembled directly from the summation of the linear absorption coefficients of three species. The systematic approach to generate the table, including the generation of the pressure-based absorption coefficient and the generation of the  $k$ -distribution, is discussed. To efficiently obtain accurate  $k$ -values for arbitrary thermodynamic states from tabulated values, a 6-D linear interpolation method is employed. A large number of radiative heat transfer calculations have been carried out to test the accuracy of the FSK look-up table. Results show that, using the FSK look-up table can provide excellent accuracy compared to the exact results. Without the time-consuming process of assembling  $k$ -distribution from individual species plus mixing, using the FSK look-up table can save considerable computational cost. To evaluate the accuracy as well as the efficiency of the FSK look-up table, radiative heat transfer via a scaled Sandia D Flame is calculated to compare the CPU execution time using the FSK method based on the narrow-band database, correlations, and the look-up table. Results show that the FSK look-up table can provide a computationally cheap alternative without much sacrifice in accuracy.

© 2015 Elsevier Ltd. All rights reserved.

### 1. Introduction

Radiative properties of molecular gases are of great importance for the study of combustion of hydrocarbon fuels and atmospheric radiation [1]. The absorption coefficient of gases, in particular for H<sub>2</sub>O and CO<sub>2</sub>, varies dramatically across most of the spectrum, which is difficult to handle in practical applications. Therefore, accurate and efficient models for gaseous radiative properties are highly desirable. The most accurate radiative approach are line-by-line (LBL) calculations, which rely on very detailed knowledge of every single spectral line [2], but require vast

amounts of computer resources and computational time [3], and remain unpractical for industrial applications. Therefore, the LBL method is used only for benchmark solutions to validate approximate methods.

An inspection of the spectral distribution of gaseous absorption coefficients reveals that the oscillatory absorption coefficients have the same value at many different wavenumbers. Recognition of this fact has led to the reordering of the absorption coefficients across the whole spectrum into a monotonic absorption coefficient distribution against normalized artificial wavenumber, which is much more efficiently integrated across the spectrum [1]. In order to treat radiation in nongray media accurately as well as efficiently, several models have been proposed based on the idea of the reordering concept, including the spectral-line-based weighted-sum-of-gray-gases (SLW)

\* Correspondence author. Fax: +209 228 4047.

E-mail address: [mmodest@eng.ucmerced.edu](mailto:mmodest@eng.ucmerced.edu) (M.F. Modest).

Nomenclature		$\Omega$	solid angle (sr)
$a$	nongray stretching function in FSK method	<i>Subscripts</i>	
$\bar{a}$	weight function in SLW method	$b$	blackbody
$C_{\text{abs}}$	molar absorption cross section ( $\text{cm}^2$ )	max	maximum
$f$	full-spectrum $k$ -distribution	min	minimum
$F_s$	absorption distribution function	$p$	pressure-based
$g$	cumulative full-spectrum $k$ -distribution or quadrature point	<i>Superscripts</i>	
$I$	radiative intensity ( $\text{W}/(\text{m}^2 \text{sr})$ )	0	reference state
$k$	$k$ -value ( $\text{cm}^{-1}$ )	<i>Abbreviations</i>	
$L$	slab width (m)	ADF	absorption distribution function
$N_{pt}$	number of nominal $k$ -values	FSK	full-spectrum $k$ -distribution
$p$	total pressure (bar)	FSCK	full-spectrum correlated $k$ -distribution
$R_u$	universal gas constant ( $\text{J}/(\text{mol K})$ )	HITEMP	high-temperature spectroscopic absorption database
$T$	temperature (K)	LBL	line-by-line
$w$	quadrature weight	RTE	radiative transfer equation
$x$	mole fraction	SLW	spectral-line-based weighted-sum-of-gray-gases
<i>Greek symbols</i>			
$\eta$	wavenumber ( $\text{cm}^{-1}$ )		
$\kappa_\eta$	spectral absorption coefficient ( $\text{cm}^{-1}$ )		
$\sigma_s$	scattering coefficient ( $\text{cm}^{-1}$ )		
$\phi$	vector of local thermodynamic state variables		
$\bar{\Phi}$	scattering phase function		

method [4], the absorption distribution function (ADF) method [5] and the full-spectrum  $k$ -distribution (FSK) method [6]. The first two, developed before the FSK, are approximate schemes, in which the absorption coefficients are reduced to a few discrete values (chosen by user), and integration over the spectrum is achieved by adding contributions from the “gray gases”.

The FSK method, on the other hand, is an exact method for homogeneous media using a continuous  $k$ -distribution over the entire spectrum. For nonhomogeneous media with variations in pressures, temperatures and species concentrations, a correlated absorption coefficient is assumed, i.e., the absorption coefficient from a thermodynamic state can essentially be correlated to that of another, resulting in the full-spectrum correlated  $k$ -distribution (FSCK) method [1]. With spectral integration performed by using high-accuracy Gauss quadrature, the FSK method can reduce the number of required radiative transfer equation (RTE) evaluations from over one million to around ten without losing spectral line information. With this obvious advantage, the FSK has become perhaps the most promising method for radiative heat transfer calculations in nongray media and has been employed in many applications. Consalvi and Liu [7] used several different spectral models to calculate radiation in axisymmetric pool fires and the results showed that the FSCK method achieves the best compromise in terms of accuracy and computational efficiency for a 34 kW pool fire. Clements et al. [8] investigated the FSK method under oxyfuel conditions and proved that the method can achieve good agreement for the test cases. Cai et al. [9]

assembled full-spectrum  $k$ -distributions from a narrow-band database and developed high fidelity radiative heat transfer models to simulate high-pressure laminar hydrogen-air diffusion flames and they also applied the FSK method to the determination of radiation in fluidized-bed coal combustion [10].

FSK results tend to be very accurate, usually being within a few percent of “exact” LBL calculations. However, the drawback of the method is that FSKs are very cumbersome to calculate. For each state, say, with three radiatively participating gases ( $\text{CO}_2$ ,  $\text{H}_2\text{O}$  and  $\text{CO}$ ) the method requires the assembly of mixture  $k$ -distributions or, for a CFD domain with several hundred thousand cells, the same amount of mixture FSKs. To overcome this drawback, Wang and Modest [11] described a narrow-band database for individual species, from which FSKs can be assembled efficiently by applying an appropriate mixing model. Cai and Modest [12] regenerated the narrow-band database using the newest HITEMP 2010 [13]. However, the mixing process for gas mixtures is computationally expensive, and creation of a single FSK for a two-gas mixture still requires between 0.0549 s to 0.469 s, depending on the mixing model [14]. Clearly, if one million FSKs are needed per time step/iteration this becomes computationally prohibitive. This has prompted the development of simple correlation formulas for individual species at atmospheric pressure [15–20], from which  $k$ -distributions can be efficiently obtained; however, their accuracy are rarely satisfactory and sometimes may lead to serious errors [14]. Recently, Pearson et al. [21, 22] tabulated ADF data (similar to FSK tabulations, except that they

use absorption cross-sections instead of absorption coefficients) for CO<sub>2</sub>, H<sub>2</sub>O and CO over the full spectrum as a tool used in the SLW method, providing an alternative to solve the radiative property of nongray gas with excellent accuracy. However, this tabulation does not include gas mixtures and is relatively coarse, making it difficult to use for mixtures.

Therefore, to improve the calculation efficiency while retaining accuracy for radiative heat transfer, an FSK look-up table for gas mixtures with  $k$ -distributions assembled directly from the summation of the linear absorption coefficients has been constructed. Examples show that the FSK look-up table can be a computationally cheap alternative without much sacrifice in accuracy.

## 2. Theoretical background

### 2.1. Full-spectrum $k$ -distributions

A full-spectrum  $k$ -distribution accounts for the variations of the Planck function and is defined as [1]

$$f_{\underline{\phi},T}(k; \underline{\phi}, T) = \frac{1}{I_b(T)} \int_0^\infty I_{b\eta}(T) \delta(k - \kappa_\eta(\underline{\phi})) d\eta \quad (1)$$

where  $\kappa_\eta$  is the absorption coefficient calculated from a spectroscopic database,  $\delta(\cdot)$  is the Dirac-delta function,  $\underline{\phi}$  is a vector of local thermodynamic state variables including pressure, temperature and species concentration,  $f_{\underline{\phi},T}(k; \underline{\phi}, T)$  is a Planck-function-weighted  $k$ -distribution with absorption coefficient evaluated at the local state  $\underline{\phi}$  and a Planck function temperature  $T$ ,  $I_b(T)$  and  $I_{b\eta}(T)$  are the Planck function and the spectral Planck function, respectively, at temperature  $T$ , and  $\eta$  is the wavenumber.

The cumulative full-spectrum  $k$ -distribution is defined as

$$g_{\underline{\phi},T}(k; \underline{\phi}, T) = \int_0^k f_{\underline{\phi},T}(k'; \underline{\phi}, T) dk' \quad (2)$$

Thus,  $g_{\underline{\phi},T}$  represents the fraction of the spectrum whose absorption coefficient lies below the value of  $k$  and therefore,  $0 \leq g_{\underline{\phi},T} \leq 1$ . Inverting Eq. (2), a smooth, monotonically increasing function  $k(g)$  can be obtained, with minimum and maximum values identical to those of  $\kappa_\eta$ .

For a nonhomogeneous mixture, the spectral variable is reordered according to the absorption coefficient at a reference state  $\underline{\phi}^0$ . Furthermore, to reduce the impact of uncorrelation, Cai and Modest [12] developed a new implementation to determine the correlated  $k$ -values. Applying this new implementation, the RTE can be reordered at the reference state  $\underline{\phi}^0$  as

$$\frac{dI_g}{ds} = k_{\underline{\phi},T}^*(g_{\underline{\phi}^0,T}) \left[ a(g_{\underline{\phi}^0,T^0}; T, T^0) I_b(T) - I_g \right] - \sigma_s(\underline{\phi}_s) \left( I_g - \frac{1}{4\pi} \int_{4\pi} I_g(s') \Phi(\underline{\phi}, s, s') d\Omega' \right) \quad (3)$$

where

$$I_g = \int_0^\infty I_\eta \delta(k - \kappa_\eta(\underline{\phi}^0)) d\eta / f_{\underline{\phi}^0,T^0}(k) \quad (4)$$

$$a \left( g_{\underline{\phi}^0,T^0}; T, T^0 \right) = \frac{f_{\underline{\phi}^0,T}(k)}{f_{\underline{\phi}^0,T^0}(k)} = \frac{dg_{\underline{\phi}^0,T}(k)}{dg_{\underline{\phi}^0,T^0}(k)} \quad (5)$$

while  $\sigma_s$  is the scattering coefficient and  $\Phi$  is the scattering phase function.

This is known as the full-spectrum correlated- $k$  (FSCK) method. Usually, the total intensity is evaluated through an  $N$ -point numerical quadrature (with quadrature points  $g_i$  and weights  $w_i$ )

$$I = \int_0^1 I_g dg_{\underline{\phi}^0,T^0} = \sum_{i=1}^N w_i I_{g_i} \quad (6)$$

and for each quadrature point  $g_i$ , Eq. (3) can be rewritten as

$$\frac{dI_{g_i}}{ds} = k^*(g_i) \left[ a(g_i) I_b(T) - I_{g_i} \right] - \sigma_s(\underline{\phi}_s) \left( I_{g_i} - \frac{1}{4\pi} \int_{4\pi} I_{g_i}(s') \Phi(\underline{\phi}, s, s') d\Omega' \right) \quad (7)$$

where  $k^*(g_i)$  is the  $k$ -value corresponding to the quadrature point  $g_i$  for a gas mixture and  $a(g_i)$  is obtained from Eq. (5).

### 2.2. Spectral-line-based weighted-sum-of-gray-gases

If Eq. (3) is integrated using a crude trapezoidal scheme, i.e., the variable absorption coefficient  $k_{\underline{\phi},T}^*(g_{\underline{\phi}^0,T})$  is replaced by a single, constant value  $\tilde{k}_i(T, \underline{\phi})$  for the  $i$ th finite range of  $F_s$  spanning across  $F_{s,i-1} < F_s \leq F_{s,i}$ , integration of Eq. (3) over the  $i$ th  $F_s$ -range leads to

$$\frac{dI_i}{ds} = \tilde{k}_i(T, \underline{\phi}) \left[ \bar{a}_i(T, T^0) I_b(T) - I_i \right] - \sigma_s(\underline{\phi}_s) \left( I_i - \frac{1}{4\pi} \int_{4\pi} I_i(s') \Phi(\underline{\phi}, s, s') d\Omega' \right), \quad i = 1, \dots, N \quad (8)$$

This is known as the spectral-line-based weighted-sum-of-gray-gases (SLW) method developed by Dension and Webb [4]. Generally, the values of  $\tilde{k}_i(T, \underline{\phi})$  and  $\bar{a}_i(T, T^0)$  are obtained from the absorption distribution function (ADF) [20–23]. Thus, the weight function  $\bar{a}_i(T, T^0)$  is evaluated from [24]

$$\bar{a}_i(T, T^0) = F_s(C_{\text{abs},i}, T, T^0) - F_s(C_{\text{abs},i-1}, T, T^0) \quad (9)$$

where  $F_s$  is the ADF and defined as

$$F_s(C_{\text{abs}}, T, T^0) = \frac{1}{I_b(T)} \sum_i \int_{\Delta\eta \in (C_{\text{abs},\eta}(T^0) < C_{\text{abs}})} I_{b\eta}(T) d\eta \quad (10)$$

The molar absorption cross section  $C_{\text{abs},\eta}$  in Eq. (10) is related to the absorption coefficient by

$$C_{\text{abs},\eta} = \frac{R_u T^0}{p x_s} \kappa_\eta \quad (11)$$

where  $R_u$  is the universal gas constant,  $p$  is the total pressure and  $x_s$  is mole fraction of species  $s$ .

As Modest and Singh [19] pointed out that the  $F_s$  in the SLW method and the  $g$  in the FSK method can be expressed using the same equation, and the SLW method

is just the crudest possible implementation of the FSK method. Therefore, the values of  $k_i(T, \phi)$  and  $\bar{a}_i(T, T^0)$  can also be obtained from the FSK look-up table developed in this paper, just replacing  $\bar{k}_i(T, \phi)$  and  $\bar{a}_i(T, T^0)$  by  $k^*(g_i)$  and  $a(g_i)$ , respectively. From this perspective, except for the order of quadrature, the SLW method is equivalent to the FSK method.

The purpose of this paper is to precalculate these  $k^*(g_i)$  and  $a(g_i)$  values for different gas mixtures and to tabulate them into an FSK look-up table for the convenience of accurate and rapid radiative calculations by using either the FSK method or the SLW method.

### 3. Construction of FSK look-up table

#### 3.1. Generation of the pressure-based absorption coefficient

In the present FSK look-up table, three species are taken into account, i.e., CO<sub>2</sub>, H<sub>2</sub>O and CO. To avoid the mixing process during FSK generation, the mixture  $k$ -distribution is generated directly from the mixture linear absorption coefficients for different thermodynamic states including all three gases, which can be expressed as

$$\kappa_\eta = (x_{\text{CO}_2}\kappa_{p\eta\text{-CO}_2} + x_{\text{H}_2\text{O}}\kappa_{p\eta\text{-H}_2\text{O}} + x_{\text{CO}}\kappa_{p\eta\text{-CO}})\cdot p \quad (12)$$

where  $x_{\text{CO}_2}$ ,  $x_{\text{H}_2\text{O}}$  and  $x_{\text{CO}}$  are the mole fractions of CO<sub>2</sub>, H<sub>2</sub>O and CO, respectively,  $p$  is the total pressure and the subscript ‘ $p$ ’ represents pressure-based absorption coefficient.

Since the linear absorption coefficient is converted from the pressure-based absorption coefficient as shown in Eq. (12), the first step in the construction of the FSK look-up table is the development of the detailed absorption spectrum as a function of relevant thermodynamic properties for the gases of interest. The detailed approach to generation of pressure-based absorption coefficients for individual species has been previously given [25], and outlined here for completeness. The HITEMP 2010 database was employed to generate the spectral pressure-based absorption coefficients, using the Voigt line profile [1] as it has been shown to have higher accuracy than the Lorentz profile for cases of sub-atmospheric pressure or high temperature where both collision and Doppler broadening are significant.

#### 3.2. Generation of the $k$ -distribution

In order to cover most conditions found in industrial practices, a large range of pressures ranging from 0.1 bar to 80 bar, temperatures ranging from 300 K to 3000 K and a full mole fraction range (from 0 to 1 for CO<sub>2</sub> and H<sub>2</sub>O, and from 0 to 0.5 for CO, which is not expected to occur at higher fractions in combustion system) is considered here. Because of both mixing and self-broadening, the  $k$ -distributions may show nonlinearities as shown in Fig. 1, in which the lines of exact  $k$ -values corresponding to different  $g$ -values may deviate from the respective linear dash-dot lines. To decrease these nonlinear effects, a large number of small mole fractions is included in the FSK look-up table. The nonlinear effects due to mixing mainly result

from the overlap of absorption bands among three species with the strongest nonlinearity appearing at low mole fractions (Fig. 1a), leading to the need of including several low mole fraction data points in the database for the generation of mixture  $k$ -distributions. In a gas mixture with CO<sub>2</sub>, CO, H<sub>2</sub>O and N<sub>2</sub>, the nonlinear effects due to self-broadening are very strong for H<sub>2</sub>O (Fig. 1b) because of the large molecule size difference between H<sub>2</sub>O and N<sub>2</sub>, plus nonlinear effects due to mixing, resulting in more mole fraction points needed for H<sub>2</sub>O to generate the  $k$ -distribution; for CO<sub>2</sub>, the size of the molecule is a little larger than N<sub>2</sub>, leading to a smaller effect of self-broadening compared to H<sub>2</sub>O, therefore, fewer mole fraction points are needed for CO<sub>2</sub> to reduce the interpolation error resulting from nonlinear effects; for CO, the molecule size is about the same size as N<sub>2</sub> and the effect of self-broadening can be ignored, thus only five mole fraction points are needed for CO to decrease the nonlinear effect due to mixing. Table 1 summarizes the pressures, gas temperatures, reference temperatures and mole fractions stored in the present FSK look-up table.

When employing Eqs. (1) and (2) to calculate the cumulative  $k$ -distributions, a set of nominal  $k$ -values between the local maximum and minimum linear absorption coefficients must be chosen for each thermodynamic state. In this work, a power distribution is used and may be expressed as [11]

$$k_i = \left[ \kappa_{\min}^\beta + \frac{i-1}{N_{pt}-1} \cdot (\kappa_{\max}^\beta - \kappa_{\min}^\beta) \right]^{1/\beta} \quad (0 < \beta < 1, 1 \leq i \leq N_{pt}) \quad (13)$$

With Eq. (13), a skewed distribution that places more points at smaller  $k$ -values is generated. After considerable numerical experimentation, a value of  $\beta = 0.1$  was found to be most satisfactory [11]. To avoid errors when the two adjacent linear absorption coefficients occur in the same  $k$ -value interval, a large number of points  $N_{pt} = 5000$  were employed. Therefore, the  $k$ -distributions obtained from LBL data can be regarded as essentially error-free.

For every thermodynamic state, the cumulative  $k$ -distribution  $g$  with 5000  $k$ -values have extremely high-accuracy; however, this leads to large storage, which is not acceptable for practical calculations. Since the cumulative  $k$ -distribution  $g$  always varies between 0 and 1, fixing the  $g$ -values is a logical choice to compact the present table. Since  $n$ -node Gauss quadrature has the highest order of accuracy, a set of the abscissas of the Gauss–Chebyshev quadrature (1) described in [11] were chosen for the fixed  $g$ -values.

To guarantee the accuracy for any optical conditions, 32 Gauss–Chebyshev quadrature points were chosen for the fixed  $g$ -values for all full-spectrum  $k$ -distributions. Thus, only the corresponding  $k$ -values and  $a$ -values were tabulated in the FSK look-up table. However, it still makes the total size of the FSK look-up table close to 5 GB. For practical applications, loading such a huge database into memory is both time-consuming and wasteful because generally only a portion of data is used for certain calculations. To avoid this drawback and also based on the fact that all records in the FSK look-up table are of the same length (there are 32 records at each thermodynamic states

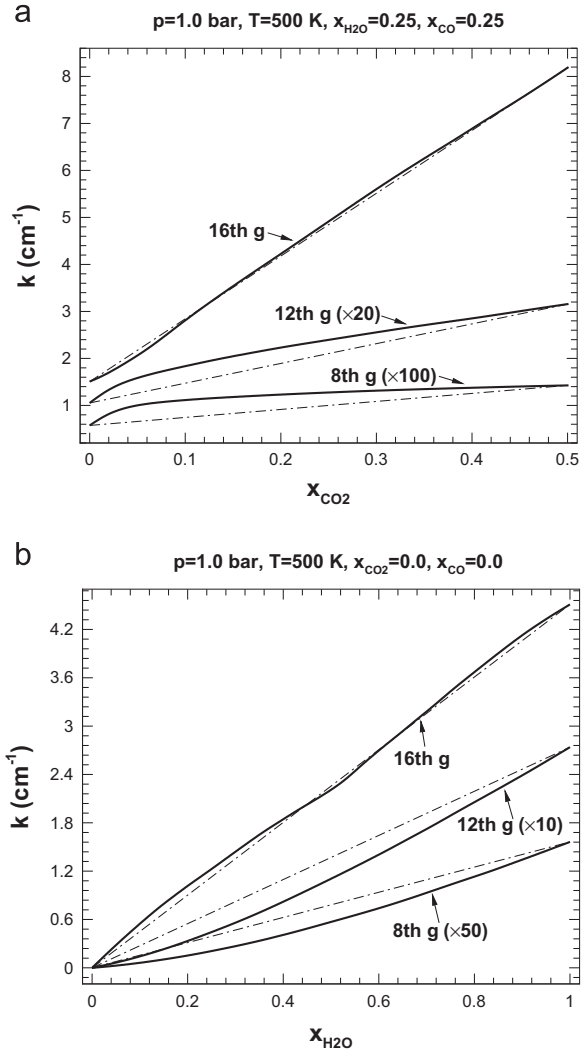


**Fig. 1.** Exact  $k$ -values corresponding to 8th, 12th and 16th  $g$ -quadrature values with increasing mole fraction using a 16-point Gauss–Chebyshev quadrature scheme [dash-dot lines represent linear interpolation lines connecting the first and last  $k$ -values; ( $\times 100$ ), ( $\times 20$ ), ( $\times 50$ ) and ( $\times 10$ ) imply amplification factors]. a. Nonlinearity due to mixing b. Nonlinearity due to self-broadening.

for both  $k$ -values and  $a$ -values), the direct data access method [11] is employed so that only the data needed by the calculations are loaded into the memory, saving both the time for reading the whole table and the memory when carrying out certain calculations. This memory management approach that guarantees the lowest memory cost without affecting the runtime efficiency during certain calculations is known as dynamic loading.

To meet the demands of different users,  $k$ -values and  $a$ -values are stored separated by both pressure and mole fraction of three species requiring 100 KB for each file. Therefore, one can assemble a small FSK look-up table for special cases; for example, a table with a single constant pressure and a mole fraction range from 0 to 0.25 can be assembled from 700 (7  $\text{CO}_2$  mole fractions  $\times$  10  $\text{H}_2\text{O}$  mole fractions  $\times$  5  $\text{CO}$  mole fractions for both  $k$ -values and  $a$ -values) individual files, leading to a table of only 68.4 MB;

**Table 1**

Precalculated thermodynamic states of FSK look-up table.

Parameters	Range	Values	Number of points
Species	$\text{CO}_2$ , $\text{H}_2\text{O}$ and $\text{CO}$		3
Pressure (total)	0.1–0.5 bar 0.7 bar 1.0–14.0 bar	Every 0.1 bar 0.7 bar Every 1.0 bar	34
Gas temperature	15.0–80 bar 300–3000 K	Every 5 bar Every 100 K	28
Reference temperature	300–3000 K	Every 100 K	28
Mole fraction of $\text{CO}_2$	0.0–0.05 0.25–1.0	Every 0.01 Every 0.25	10
Mole fraction of $\text{H}_2\text{O}$	0.0–0.05 0.1–0.2 0.25–1.0	Every 0.01 Every 0.05 Every 0.25	13
Mole fraction of $\text{CO}$	0.0–0.5	[0.0, 0.01, 0.05, 0.1, 0.25, 0.5]	6

furthermore, for RTE evaluations, usually 8–16 quadrature points are sufficient, making the size of the table even smaller, for example, a table with a single constant pressure with 16 quadrature points is only 34.2 MB in size.

### 3.3. Interpolation method

For an arbitrary thermodynamic state, a full-spectrum  $k$ -distribution is specified by pressure, gas temperature, reference temperature and three concentrations. Therefore, a six-dimensional interpolation method is required to obtain the full-spectrum  $k$ -distribution from the look-up table. To achieve relatively small computational cost, the simplest and fastest 6-D linear interpolation method with a  $2 \times 2 \times 2 \times 2 \times 2 \times 2$  domain is employed to obtain both  $k$ -values and  $a$ -values. Since both gas and reference temperature ranges are equally spaced, the domain values of these two parameters can be directly obtained; while the domain values of pressure and three species need to be searched due to the unequally spaced ranges, requiring some extra computational time.

Since the effect of self-broadening is remarkably larger at both high-pressure and low temperature, especially for  $\text{H}_2\text{O}$ , it is appropriate to compare the negative radiative heat source  $\nabla \cdot q$  calculated by two mixture  $k$ -distributions obtained from different sources to test the accuracy of 6-D linear interpolation. As shown in Fig. 2, the  $k$ -distributions shown as a red dash-dot line are obtained from 6-D linear interpolation among the tabulated values in the FSK look-up table; and the  $k$ -distributions shown as a black solid line are calculated by an exact FSK, for which the  $k$ -distributions are directly calculated from the LBL absorption coefficient database [25]. It can be seen that two values of  $\nabla \cdot q$  are in excellent agreement at both high-pressure and high temperature, and the maximum error stays around 2%. Therefore, the 6-D linear interpolation method was deemed good enough to obtain the  $k$ -values from the FSK look-up table.

## 4. Results and discussions

### 4.1. Sample calculations

#### 4.1.1. Accuracy investigation

To test the accuracy of the FSK look-up table, a large number of sample calculations were carried out for one-dimensional slabs of a homogeneous gas mixture bounded by cold black walls, with  $\nabla \cdot q$  predicted by the FSK method using the look-up table. Since the FSK method is exact for homogeneous media, the reference solution is provided by the exact FSK. Thus, any error generated by using the FSK look-up table is due to inaccuracies from interpolation of  $k$ -distributions from the FSK look-up table. For these cases, the analytical solution of the RTE exists [1] and is used for comparison. Mixtures of three species ( $\text{CO}_2$ ,  $\text{H}_2\text{O}$ , and  $\text{CO}$ ) in different thermodynamic states are shown in Table 2. All FSK calculations employ a 16-point Gauss–Chebyshev scheme.

Figs. 3 through 5 show the representative curves of  $\nabla \cdot q$  across the slab varying with pressures, temperatures and slab widths, respectively. For better readability, only FSK exact results and errors made by database-assembled  $k$ -distribution calculations from the FSK look-up table have been plotted. Fig. 3 shows the effects of total pressure on overall accuracy, keeping all other parameters fixed. For low pressures such as 0.85 bar,  $\nabla \cdot q$  is essentially constant across the slab, since the gas is so optically thin that all

emission escapes from the medium without self-absorption. For high pressures, the gas becomes optically thick and, therefore, energy emitted near the center cannot escape, leading to the strong gradients toward the boundaries. The same phenomenon can be also seen in Fig. 4, in which the temperature  $T$  is increased, and in Fig. 5, in which the slab width  $L$  is increased. For all cases, the maximum error across the slab stays around or below 2%, implying that the FSK look-up is sufficiently accurate for radiative calculations.

#### 4.1.2. Efficiency investigation

To test the efficiency of the FSK look-up table, CPU times of generating  $k$ -distributions for arbitrary gas mixtures at arbitrary thermodynamic states are compared using FSK generation based on exact FSK, assembly from the narrow-band database [12], from correlations [18, 19] and from the look-up table developed in this paper, respectively. Since the correlations can be used only at 1 bar, the pressure for all arbitrary  $k$ -distributions is fixed to 1 bar. The temperature range for arbitrary thermodynamic states is 300–3000 K. Three gases ( $\text{CO}_2$ ,  $\text{H}_2\text{O}$  and  $\text{CO}$ ) with mole fractions ranging from 0 to 0.25 are included in the generation of arbitrary  $k$ -distributions. However, correlations are only available for  $\text{CO}_2$  and  $\text{H}_2\text{O}$ ; therefore, the  $k$ -distributions generated using correlations include only two gases.

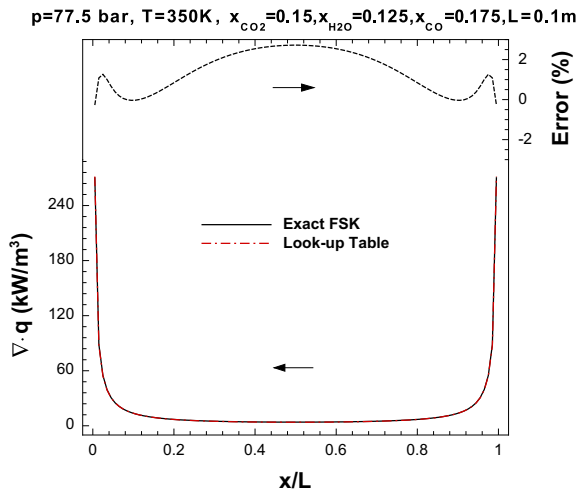


Fig. 2. Comparison of calculated by  $k$ -distributions obtained by an exact evaluation and 6-D linear interpolation from tabulated data in the FSK look-up table; 16-point quadrature.

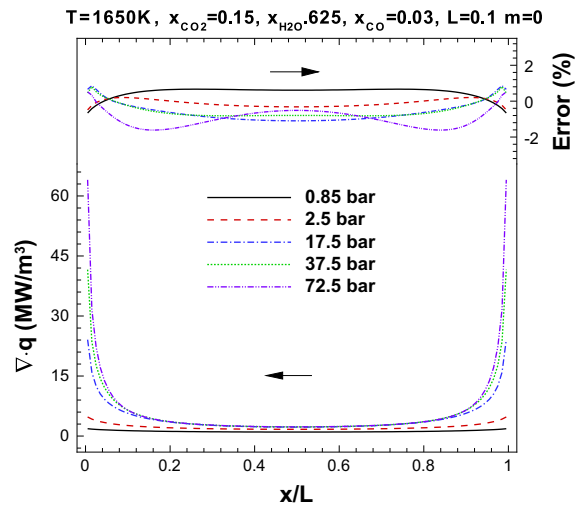


Fig. 3. Negative radiative heat source for a 15.0%  $\text{CO}_2$ –62.5%  $\text{H}_2\text{O}$ –3%  $\text{CO}$ –19.5%  $\text{N}_2$  mixture at varying pressures; 16-point quadrature.

Table 2

Investigated gas mixture states and corresponding fixed parameters.

Investigated gas mixture states	Fixed parameters						
	$p$ (bar)	$T$ (K)	$x_{\text{CO}_2}$	$x_{\text{H}_2\text{O}}$	$x_{\text{CO}}$	$x_{\text{N}_2}$	$L$ (m)
$p$ (bar)	0.85, 2.5, 17.5, 37.5, 72.5	–	0.150	0.625	0.030	0.195	0.1
$T$ (K)	450, 1050, 1650, 2250, 2850	17.5	0.375	0.375	0.075	0.175	0.1
$L$ (m)	0.001, 0.01, 0.1, 0.5, 1	17.5	0.625	0.125	0.175	0.075	–

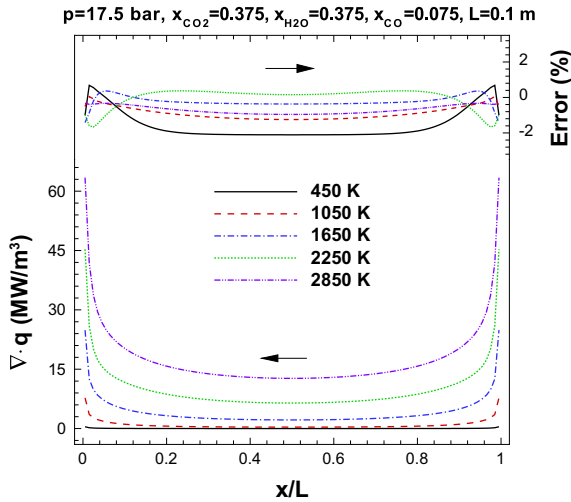


Fig. 4. Negative radiative heat source for a 37.5% CO<sub>2</sub>–37.5% H<sub>2</sub>O–7.5% CO–17.5% N<sub>2</sub> mixture at varying temperatures; 16-point quadrature.

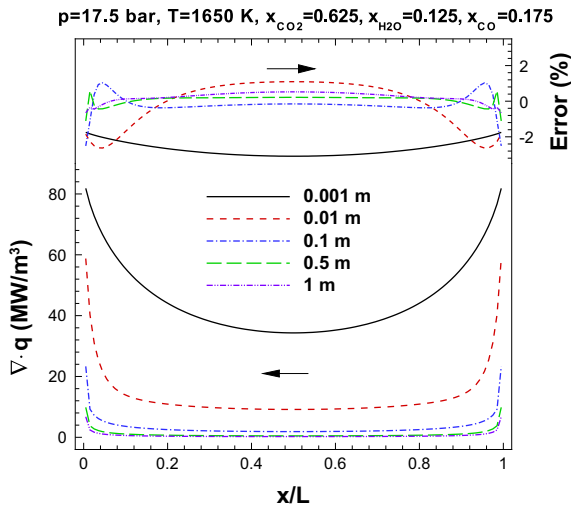


Fig. 5. Negative radiative heat source for a 62.5% CO<sub>2</sub>–12.5% H<sub>2</sub>O–17.5% CO–7.5% N<sub>2</sub> mixture at varying slab thicknesses; 16-point quadrature.

Table 3

CPU time comparisons of generating 10,000 arbitrary  $k$ -distributions based on different databases.

Database	Mixing model	CPU (s)
Exact FSK	–	31216
Narrow-band	Multiplication	1390
	MRmixing	5905
Correlations	Multiplication	0.41
	MRmixing	8.97
Look-up table	–	0.26

Table 3 shows CPU time comparisons for generating 10,000 arbitrary  $k$ -distributions based on four different databases. Two mixing models are included in the comparisons for the  $k$ -distributions assembly from both the narrow-band database and correlations, i.e., the multiplication model [26] and the Modest and Riazzi mixing (MRmixing) model

[27]. Since the exact FSK is calculated from the LBL absorption coefficient database, the required CPU time for generation using the exact FSK, while large, is considerably lower than that when calculated directly from HITEMP 2010. Using the narrow-band database saves considerable CPU time because  $k$ -distributions have been precalculated for individual species. However, CPU time of generation using the narrow-band database is still large due to the mixing process. As listed in Table 3, even employing the more efficient but less accurate multiplication model, using the narrow-band database still requires 1390 s to generate 10,000 arbitrary  $k$ -distributions. CPU time for generation using correlations is much smaller than that using the narrow-band database; it also depends on the mixing model: CPU time employing the MRmixing model is much larger than that for the multiplication model. Without both assembly of  $k$ -distributions and mixing, CPU time using the look-up table is remarkably cheap, which is even faster than that using correlations with the more rapid multiplication model.

Comparisons of  $k$ -distributions calculated from different databases in Table 3 at one thermodynamic state are shown in Fig. 6 (left). The  $k$ -distributions calculated from both narrow-band database with MRmixing model and look-up table overlap very well with the exact results, which are directly calculated by exact FSK. By contrast, those  $k$ -distributions calculated from the narrow-band database with the multiplication model and from correlations with the two different mixing models show some discrepancies compared to the exact results. Employing those  $k$ -distributions, the negative radiative heat source and errors compared to exact FSK results across the 1D slab are shown in Fig. 6 (right). It is clear that with accurate  $k$ -distributions, the results using the narrow-band database with the MRmixing model and the look-up table are much better than those using the correlations and/or the multiplication mixing model, showing less than 2% error across the slab compared to exact FSK results. In addition, comparing the CPU times shown in Table 3 makes it clear that the look-up table is a more appropriate way for radiative calculations than using the narrow-band database with the MRmixing model.

#### 4.2. Flame calculation

In order to evaluate accuracy and efficiency of the FSK look-up table, radiation from a realistic flame is considered. The flame is derived from Sandia Flame D [28] by artificially quadrupling the jet diameter, resulting in strong radiation effects that are found in practical combustion configurations. The flame is simulated on a two-dimensional axisymmetric mesh, and only the quasi-steady time-averaged temperature and species mass fraction fields shown in Fig. 7 are used here for radiation calculation comparisons. Hence, no turbulence-radiation interaction is considered, and  $\nabla \cdot q$  is determined using the FSK method based on three different databases (narrow-band, correlations and look-up table) without feedback to the flame. The RTE is solved by the  $P_1$  method. The total pressure is 1 bar and three species (CO<sub>2</sub>, H<sub>2</sub>O and CO) are included in the calculations except for the calculations using the correlations, which contains only CO<sub>2</sub> and H<sub>2</sub>O.



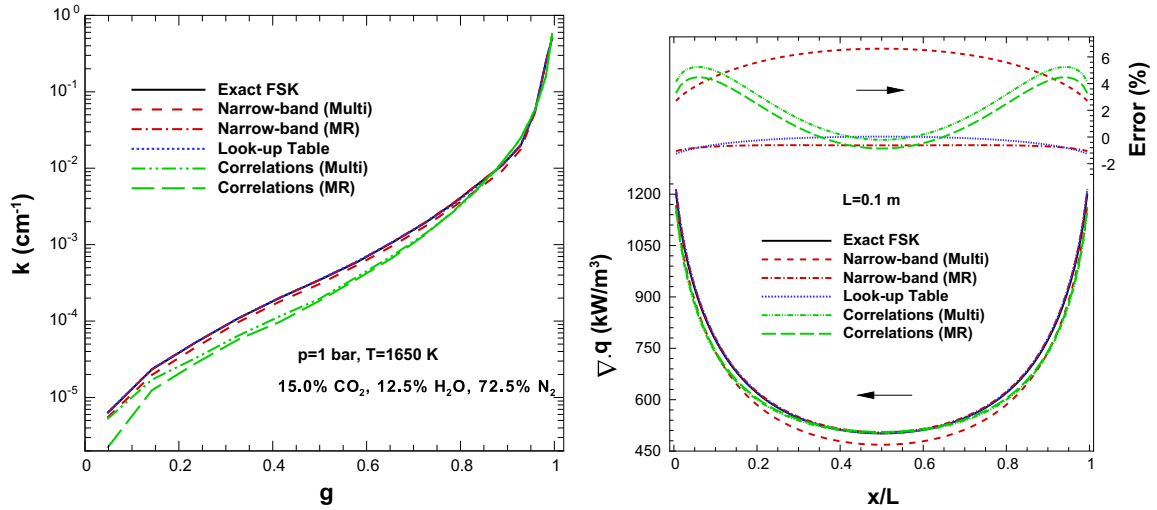


**Fig. 6.**  $k$ -distributions for a gas mixture (left) and corresponding negative radiative heat source and errors compared to exact FSK for a 1D slab (right) using different databases; 16-point quadrature.

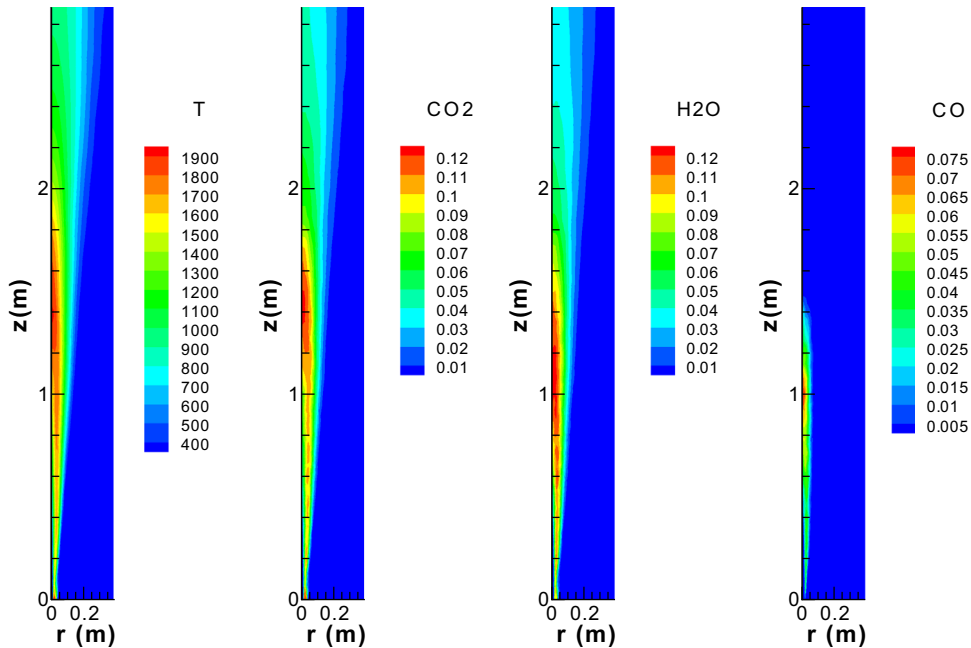


**Fig. 7.** Time-averaged spatial profile of temperature, CO<sub>2</sub> mass fraction, H<sub>2</sub>O mass fraction and CO mass fraction of enlarged Sandia Flame D. (For interpretation of the colors in this figure, the reader is referred to the web version of this article).

All FSK calculations employ a 16-point Gauss–Chebyshev quadrature scheme and are compared with LBL calculations at three downstream locations.

The results using the narrow-band database employed the MRmixing model have been presented by Cai and Modest [12]. As shown in Fig. 8, at all three locations, using the narrow-band database with the MRmixing model provides excellent performance compared to LBL results. The discrepancies between the results from the narrow-band database with the MRmixing model and LBL results mainly come from the quadrature errors, interpolation errors and mixing errors. When employing the quicker

multiplication model, the accuracy using the narrow-band database dramatically decreases due to the increase of mixing errors. Calculations using the correlations with either multiplication model or MRmixing model show the worst performance among the three databases. Since radiation of CO is not very dominant, the large discrepancies between the correlation results and LBL results are mainly due to the inaccurate  $k$ -distributions obtained from the correlations. Without mixing, only quadrature errors and interpolation errors are present when using the look-up table. Since the quadrature errors are very tiny when employing 16-point quadrature and the

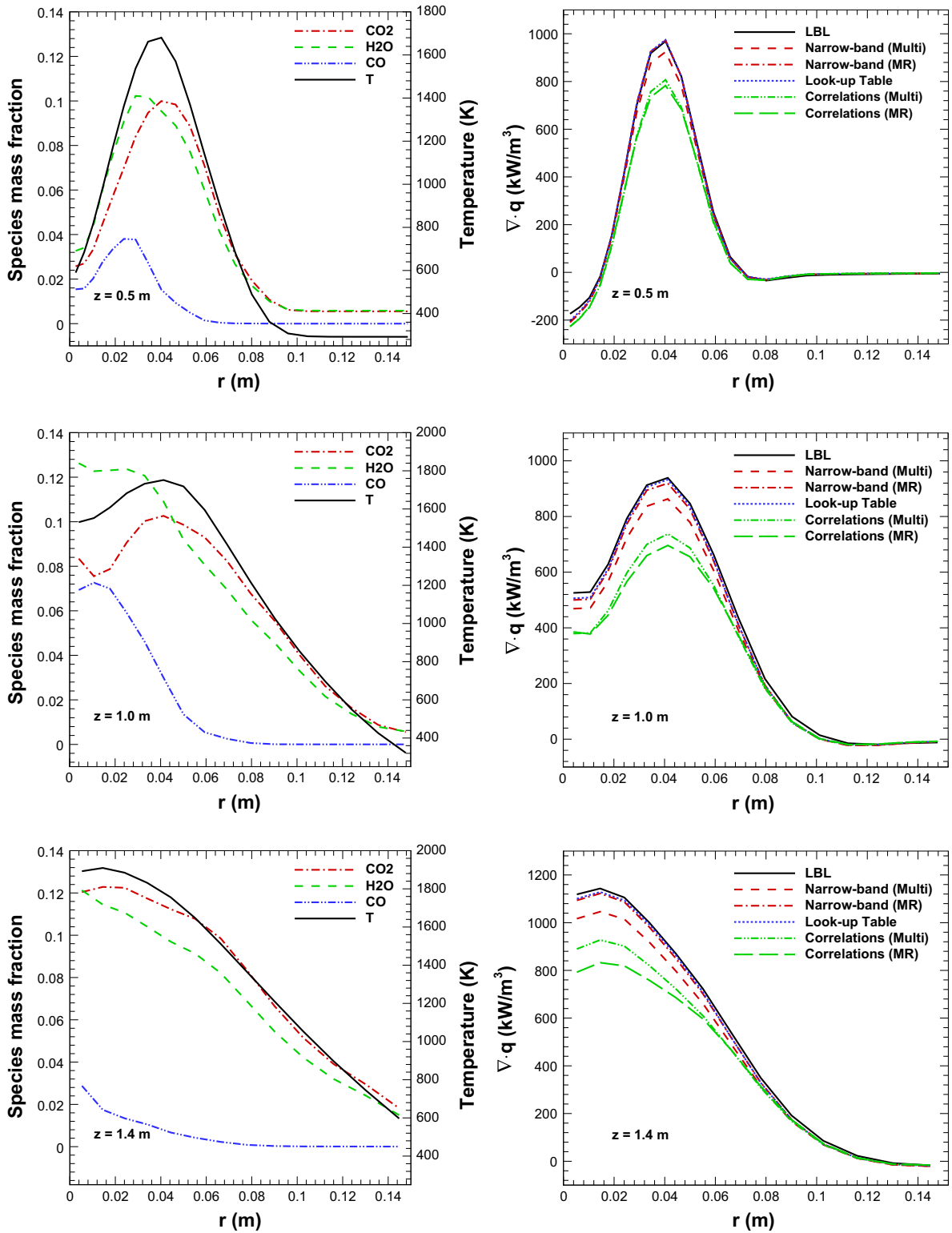


Fig. 8. Comparisons of FSK calculations using different databases (right column) along with the species mass fraction and the temperature (left column) at three locations,  $z=0.5$  m (top),  $z=1.0$  m (middle), and  $z=1.4$  m (bottom); Multi: multiplication model, MR: MRmixing model.

**Table 4**

Comparison of CPU times for calculations of the Sandia D flame case using different databases.

Database	Mixing model	CPU (s)
LBL	–	87331.98
Narrow-band	Multiplication	1513.57
	MRmixing	8422.88
Correlations	Multiplication	1.76
	MRmixing	13.34
Look-up table	–	1.56

interpolation errors are around 2% as shown in Section 4.1, calculations using the look-up table are very close to the LBL results, showing almost the best performance among three databases. At the locations where radiation is dominated by the emission, e.g.  $z=0.5$  m and  $z=1.0$  m, calculations using the look-up table even overlap with LBL results. This illustrates that in practical applications using the look-up table can achieve a LBL accuracy in predicting of radiative heat source.

CPU times of the LBL calculations and the FSK calculations using the three databases are compared in Table 4. Because of the one million evaluations of the RTE, using the LBL database requires a large amount of CPU time. Using the narrow-band database can save much CPU time compared to LBL calculations. However, even employing the more rapid multiplication model, the CPU time using the narrow-band database is still about a factor of 970 higher than that using the look-up table due to the assembly of mixture  $k$ -distributions from individual species. Thus, for a single calculation without feedback, it is quite time-consuming to use the narrow-band database in practical applications. When employing dynamic loading, considerable time for reading the whole look-up table into memory is saved, making the CPU time using the look-up table even shorter than that using correlations with the multiplication model. Therefore, together with the accuracy discussions above, using the look-up table appears to be a better alternative for radiative calculations, and is computationally cheaper than using correlations but with high-accuracy, which is even better than using the narrow-band database.

## 5. Conclusions

To avoid the time-consuming process of assembling mixture full spectrum  $k$ -distributions from spectroscopic databases plus mixing, an FSK look-up table has been constructed, from which  $k$ -distributions can be obtained by interpolation. The following conclusions are drawn from this work:

1. The FSK look-up table presented in this paper includes three species ( $\text{CO}_2$ ,  $\text{H}_2\text{O}$  and  $\text{CO}$ ) and has a large range of pressures ranging from 0.1–80 bar and temperatures ranging from 300–3000 K. For both  $\text{CO}_2$  and  $\text{H}_2\text{O}$ , the considered mole fraction range is between 0 and 1; while for  $\text{CO}$ , it is between 0 and 0.5.
2. A large number of calculations were carried out to investigate the effects of total pressure, temperature and slab width on the accuracy of the FSK look-up table. It was demonstrated that the full-spectrum  $k$ -distributions of the gas mixture at arbitrary thermodynamic states can be obtained accurately from the FSK look-up table by 6-D linear interpolation scheme presented in the paper.
3. The major advantage of the FSK look-up table is efficiency, requiring CPU time that is even cheaper than that using correlations with the simple (and least accurate) rapid multiplication model but achieving almost the same accuracy as using the LBL database. Considering both accuracy and efficiency, the FSK look-up table appears to be a very effective tool for practical applications. The look-up database is available from the corresponding author's website upon request at <http://eng.ucmerced.edu/people/mmodest>.

## Acknowledgments

This work was supported by the NSF/DOE Collaborative Research Award No. 1258635. The first author acknowledges sponsorship by the China Scholarship Council.

## References

- [1] Modest MF. Radiative heat transfer. 3rd ed.. New York: Academic Press; 2013.
- [2] Arnold JO, Whiting EE, Lyle GC. Line-by-line calculation of spectra from diatomic molecules and atoms assuming a voigt line profile. J Quant Spectrosc Radiat Transf 1969;9(6):775–98.
- [3] Ma J, Li BW, Howell JR. Thermal radiation heat transfer in one- and two-dimensional enclosures using the spectral collocation method with full-spectrum  $k$ -distribution model. Int J Heat Mass Transf 2014;71:35–43.
- [4] Denison MK, Webb BW. A spectral line-based weighted-sum-of-gray-gases model for arbitrary RTE solvers. ASME J Heat Transf 1993;115(4):1004–12.
- [5] Pierrot L, Rivière P, Soufiani A, Taine J. A fictitious-gas-based absorption distribution function global model for radiative transfer in hot gases. J Quant Spectrosc Radiat Transf 1999;62(5):609–24.
- [6] Modest MF. Narrow-band and full-spectrum  $k$ -distributions for radiative heat transfer-correlated- $k$  vs. scaling approximation. J Quant Spectrosc Radiat Transf 2003;76(1):69–83.
- [7] Consalvi JL, Liu F. Radiative heat transfer in the core of axisymmetric pool fires-I: evaluation of approximate radiative property models. Int J Therm Sci 2014;84:104–17.
- [8] Clements AG, Porter R, Pranzitelli A, Pourkashanian M. Evaluation of FSK models for radiative heat transfer under oxy fuel conditions. J Quant Spectrosc Radiat Transf 2015;151:67–75.
- [9] Cai J, Lei SH, Dasgupta A, Modest MF, Haworth DC. High fidelity radiative heat transfer models for high-pressure laminar hydrogen-air diffusion flames. Combust Theory Model 2014;18(6):607–26.
- [10] Cai, J, Modest, MF. Radiation modeling in fluidized-bed coal combustion. In: Proceedings of the 50th AIAA aerospace sciences meeting including the new horizons forum and aerospace exposition. Tennessee, USA; Jan 9–12, 2012.
- [11] Wang AQ, Modest MF. High-accuracy, compact database of narrow-band  $k$ -distributions for water vapor and carbon dioxide. J Quant Spectrosc Radiat Transf 2005;93(1):245–61.
- [12] Cai J, Modest MF. Improved full-spectrum  $k$ -distribution implementation for inhomogeneous media using a narrow-band database. J Quant Spectrosc Radiat Transf 2014;141:65–72.
- [13] Rothman LS, Gordon IE, Barber RJ, Dothe H, Gamache RR, Goldman A, et al. HITEMP, the high-temperature molecular spectroscopic database. J Quant Spectrosc Radiat Transf 2010;111(15):2139–50.

- [14] Cai J, Marquez R, Modest MF. Comparisons of radiative heat transfer calculations in a jet diffusion flame using spherical harmonics and  $k$ -distributions. *ASME J Heat Transf* 2014;136(11):112702–1–9.
- [15] Denison MK, Webb BW. An absorption-line blackbody distribution function for efficient calculation of total gas radiative transfer. *J Quant Spectrosc Radiat Transf* 1993;50:499–510.
- [16] Denison MK, Webb BW. Development and application of an absorption line blackbody distribution function for CO<sub>2</sub>. *Int J Heat Mass Transf* 1995;38:1813–21.
- [17] Zhang H, Modest MF. Full-spectrum  $k$ -distribution correlations for carbon dioxide mixtures. *J Thermophys Heat Transf* 2003;17(2): 259–63.
- [18] Modest MF, Mehta RS. Full-spectrum  $k$ -distribution correlations for CO<sub>2</sub> from the CDSD-1000 spectroscopic databank. *Int J Heat Mass Transf* 2004;47:2487–91.
- [19] Modest MF, Singh V. Engineering correlations for full spectrum  $k$ -distribution of H<sub>2</sub>O from the HITEMP spectroscopic databank. *J Quant Spectrosc Radiat Transf* 2005;93:263–71.
- [20] Liu F, Chu H, Zhou H, Smallwood GJ. Evaluation of the absorption line blackbody distribution function of CO<sub>2</sub> and H<sub>2</sub>O using the proper orthogonal decomposition and hyperbolic correlations. *J Quant Spectrosc Radiat Transf* 2013;128:27–33.
- [21] Pearson JT, Webb BW, Solovjov VP, Ma J. Effect of total pressure on the absorption line blackbody distribution function and radiative transfer in H<sub>2</sub>O, CO<sub>2</sub>, and CO. *J Quant Spectrosc Radiat Transf* 2014;143:100–10.
- [22] Pearson JT, Webb BW, Solovjov VP, Ma J. Efficient representation of the absorption line blackbody distribution function for H<sub>2</sub>O, CO<sub>2</sub>, and CO at variable temperature, mole fraction, and total Pressure. *J Quant Spectrosc Radiat Transf* 2014;138:82–96.
- [23] Węcel G, Ostrowski Z, Kozoń P. Absorption line black body distribution function evaluated with proper orthogonal decomposition for mixture of CO<sub>2</sub> and H<sub>2</sub>O. *Int J Numer Methods Heat Fluid Flow* 2014;24(4):932–48.
- [24] Modest MF. The treatment of nongray properties in radiative heat transfer: from past to present. *ASME J Heat Transf* 2013;135 061801–061.
- [25] Wang AQ. Investigation of turbulence-radiation interaction in turbulent flames using a hybrid finite volume/Monte Carlo approach (dissertation). University Park (PA): Pennsylvania State University; 2007.
- [26] Solovjov VP, Webb BW. SLW modeling of radiative transfer in multicomponent gas mixtures. *J Quant Spectrosc Radiat Transf* 2000;65:655–72.
- [27] Modest MF, Riazzri RJ. Assembly of full-spectrum  $k$ -distributions from a narrow-band database: effects of mixing gases, gases and nongray absorbing particles, and mixtures with nongray scatterers in nongray enclosures. *J Quant Spectrosc Radiat Transf* 2005;90(2): 169–89.
- [28] Pal G, Gupta A, Modest MF, Haworth, DC. Comparison of accuracy and computational expense of radiation models in simulation of non-premixed turbulent jet flames. In: Proceedings of the ASME/JSME 2011 8th thermal engineering joint conference. Honolulu, Hawaii, USA; Mar 13–17, 2011.